

# Dioscin attenuates high-fat diet-induced insulin resistance of adipose tissue through the IRS-1/PI3K/Akt signaling pathway

HAIJUAN LI<sup>1\*</sup>, LIANZHI YU<sup>2\*</sup> and CHANGSHENG ZHAO<sup>3</sup>

<sup>1</sup>Department of Clinical Nutrition; <sup>2</sup>Health Check Centre,

The Affiliated Yantai Yuhuangding Hospital of Qingdao University, Yantai, Shandong 264000;

<sup>3</sup>Department of Nutrition, The Second Hospital of Shandong University, Jinan, Shandong 250033, P.R. China

Received February 27, 2018; Accepted October 10, 2018

DOI: 10.3892/mmr.2018.9700

**Abstract.** Insulin resistance, as a common metabolic disorder, may be caused by diet-induced obesity. The aim of the present study is to investigate the effects of dioscin on regulating insulin resistance of adipose tissue induced by a high-fat diet (HFD). An animal model was established successfully using C57BL/6J mice with high-fat feeding, followed by treatment with 5, 10 and 20 mg/kg dioscin through gavage for 18 weeks, and randomly divided into a control group, a HFD model group and a dioscin group treated with 5, 10 and 20 mg/kg/day dioscin for 12 weeks. Histopathological changes in adipose tissues were examined using hematoxylin and eosin staining. Biochemical parameters of the serum were also monitored, including glucose, insulin, total triglyceride, homeostasis model assessment of insulin resistance (HOMA-IR) and adipose insulin resistance (Adipo-IR) levels. Expression of the mRNA and associated proteins of the insulin receptor substrate 1 (IRS-1)/phosphoinositide 3-kinase (PI3K)/protein kinase B (Akt) pathways were determined using reverse transcription-quantitative polymerase chain reaction (RT-qPCR) and western blot analysis, respectively. HOMA-IR and Adipo-IR values of mice fed with a HFD were significantly higher compared with those in the control group ( $P<0.01$ ). However, dioscin administration significantly decreased HOMA-IR and Adipo-IR values in a dose-dependent manner ( $P<0.05$ ), suggesting the effects of dioscin on attenuating insulin resistance. RT-qPCR results indicated that the associated genes of the IRS-1/PI3K/Akt pathway were significantly downregulated by HFD compared with the control group ( $P<0.05$ ), while dioscin significantly increased

the expression of those genes compared with the control group ( $P<0.05$ ). Similarly, the significant increase in phosphorylated (p-)IRS-1/IRS-1 ( $P<0.05$ ) and p-Akt/Akt ( $P<0.05$ ) values were substantially reversed by dioscin treatment. Dioscin pronouncedly mitigated insulin resistance in adipose tissues through the IRS-1/PI3K/Akt pathway and has potential to be used as a novel therapeutic agent for the therapy of HFD-induced insulin resistance in adipose tissue.

## Introduction

Insulin resistance, one of the major pathogenic events in type-2 diabetes mellitus, is characterized by the inertness of tissues for insulin regulation (1). Insulin resistance impairs glucose uptake in the peripheral tissue and increases hepatic glucose output. In 2013, Turner *et al* (2) reported that diet-induced obesity substantially increased the risk of insulin resistance. In obese states, the excessive secretion of free fatty acids (FFA) and adipokines result in endocrine effects to further lower insulin sensitivity in muscle and liver (2). Rodents fed with a high-fat diet (HFD) frequently develop obesity and insulin resistance, providing the potential to study the development of this disease, and investigate novel treatments to mitigate the disease-associated complications (2). Thus far, a number of plant-derived compounds have demonstrated hypoglycemic properties and the potential to ameliorate insulin resistance associated with obesity.

Dioscin, as a plant-derived steroidal saponin, is abundant in *Dioscorea* species (yams) which has traditionally been used for the treatment of asthma, abscesses, chronic diarrhea and ulcers (3). Extracts of *Dioscorea batatas* were additionally revealed to ameliorate the insulin resistance of mice fed with a HFD (4). Dioscin has a wide spectrum of biological activities, including anti-cancer (5) and antiviral activities (6). Meanwhile, it is also used for the management of hyperglycemia and dyslipidemia due to its cardiovascular protective activity (7). In addition, the functions in reducing oxidative stress and inflammatory responses have been exploited to attenuate ischemic-reperfusion injuries in multiple organs (8). Previous evidence indicates that dioscin has potent effects against obesity in mice (9), in which dioscin was able to alleviate the increased body weight and liver lipid accumulation. Given that a HFD and obesity are important contributors to

**Correspondence to:** Dr Changsheng Zhao, Department of Nutrition, The Second Hospital of Shandong University, 247 Beiyuan Avenue, Jinan, Shandong 250033, P.R. China  
E-mail: zhaodocsci@hotmail.com

\*Contributed equally

**Key words:** dioscin, insulin tolerance, high-fat diet, insulin receptor substrate 1/phosphoinositide 3-kinase/protein kinase B pathway

insulin resistance, dioscin is a promising drug for the treatment of insulin resistance induced by a HFD.

The hyperactivity of stress-associated and inflammatory pathways is a common characteristic of insulin-resistant adipose tissues (10). Signaling pathways involved in oxidative stress and inflammatory responses, including the phosphoinositide 3-kinase (PI3K)/protein kinase B (Akt) signaling pathway, have been considered as targets to reduce insulin resistance (11). Gallagher *et al* (12) reported that the suppression of PI3K induced hyperglycemia in a mouse with insulin resistance and hyperinsulinemia, suggesting that drugs restoring the activity of PI3K may potentially alleviate insulin resistance. In fact, the roles of dioscin in modulating the PI3K/Akt pathway have already been demonstrated in 2013 (13).

Based on this, the present study aimed to corroborate the effect of dioscin on regulating insulin resistance induced by a HFD. The ability of dioscin in modulating phenotypic parameters of the serum, including glucose, triglyceride (TG) and total cholesterol (TC) levels, was investigated. To ascertain the regulatory mechanism of dioscin, the involvement of the insulin receptor substrate 1 (IRS-1)/PI3K/Akt signaling pathway and peroxisome proliferator-activated receptor  $\gamma$  (PPAR- $\gamma$ ) pathway were characterized. Furthermore, factors associated with fatty acid synthesis, including fatty acid synthetase (FAS) and sterol regulatory element-binding protein 1 (SREBP-1c; a transcription factor that activates fatty acid synthesis) and the adipocyte-derived insulin-sensitizing protein adiponectin were monitored. Considering the prevalence of insulin resistance and the critical need for an effective drug to ameliorate this disease, the results of the present study may verify dioscin as an effective drug to restore the insulin sensitivity of adipose tissues.

## Materials and methods

**Animals.** All animal experiments were performed and ethically approved by the Animal Care and Use Committee of the The Affiliated Yantai Yuhuangding Hospital of Qingdao University (Yantai, China). A total of 50 healthy male C57BL/6J mice (20–23 g) aged 6 weeks were purchased from Nanjing Junke Biological Engineering Co., Ltd. (Nanjing, China; <http://njjkswg.china.herostart.com/>). Regular food (10% kcal from fat, 70% kcal from carbohydrates) and high-fat food (60% kcal from fat, 20% kcal from carbohydrates) were purchased from Research Diets, Inc. (New Brunswick, NJ, USA). Mice were housed in a specific pathogen-free room at 22–25°C and 40–50% humidity under a 12 h light-dark cycle and had *ad libitum* access to food and water.

The animals were allowed to adapt for 7 days prior to being randomized into five groups: A control group (n=10) receiving regular food and treated with saline through gavage; a HFD group (n=10) were fed with a HFD and treated with saline through gavage; and dioscin treatment groups treated with a HFD and 5 mg/kg/day (low), 10 mg/kg/day (medium) or 20 mg/kg/day (high) dioscin through gavage. Over 12 weeks, body weight and body fat were recorded. Subsequent to the end of the 12 weeks, the mice were fasted for 1 day and blood was collected for serum biochemical analysis. Then mice were then sacrificed in a CO<sub>2</sub> chamber. Adipose tissues were harvested, washed with saline, fixed

in 10% formalin at 4°C for 1 h and stored frozen in liquid nitrogen until use.

**Serum biomedical analysis.** Total TG, TC and glucose levels in serum were measured using enzyme-linked immunosorbent assay kits (Shanghai Kexin Biotechnology, Co., Ltd., Shanghai, China) according to the manufacturer's protocol. The absorbance was measured using a plate reader (Molecular Devices, LLC, Sunnyvale, CA, USA) at a wavelength of 510 nm.

**Determination of adiposity, homeostasis model assessment of insulin resistance (HOMA-IR) and adipose insulin resistance (Adipo-IR) levels.** The following equations were used to determine the adiposity, HOMA-IR and Adipo-IR levels of the mice:

$$\text{Adiposity index} = (\text{body fat}/\text{final body mass}) \times 100$$

$$\text{HOMA-IR} = [\text{insulin level subsequent to fasting } (\mu\text{IU/ml}) \times \text{glucose level following fasting (mM)}] / 22.5$$

$$\text{Adipo-IR} = \text{insulin level subsequent to fasting (mmol/l)} \times \text{non-esterified fatty acids (NEFA) level following fasting (pmol/l)}$$

**Reverse transcription-quantitative polymerase chain reaction.** Total RNA in the adipose tissues was isolated using a TRIzol kit (Thermo Fisher Scientific, Inc., Waltham, MA, USA). Synthesis of cDNA was performed using a PrimeScript RT reagent kit with gDNA Eraser (Takara Biotechnology Co., Ltd., Dalian, China). These kits were used according to the manufacturers' protocols. PCR reaction conditions were as follows: 95°C for 5 min, and 40 cycles of 95°C for 20 sec, 60°C for 30 sec and 72°C for 30 sec. PCR was performed using a CFX96 Real Time PCR detection system (Bio-Rad Laboratories, Inc., Hercules, CA, USA) with SYBR green II. Primers used for RT-qPCR are described in Table I.  $\beta$ -actin was used as an internal control. Quantification of the mRNA level was performed using the 2<sup>−ΔΔC<sub>q</sub></sup> method (14).

**Hematoxylin and eosin (H&E) staining.** Adipose tissues were harvested from the mice, fixed with 10% formalin at 4°C for 24 h, and embedded in paraffin at 60°C for 1 h. The tissue block was sectioned at a thickness of 5  $\mu$ m. The tissue was dewaxed twice with xylene for 15 min at 24°C. Following hydration by passing a series of graded ethanol concentrations (95% ethanol for 5 min, 90% ethanol for 5 min, 70% ethanol for 2 min and distilled water for 5 min). Tissues were then stained using hematoxylin and 0.5% eosin (H&E) (Nanchang Yulu Experimental Equipment Co., Ltd., Jiangxi, China; <http://shop1379475340812.cn.makepolo.com/>) at room temperature for 10 min, followed by dehydration and covering with a thin glass. The morphology of the adipose tissue was examined under a light microscope (magnification, x200; Olympus Corporation, Tokyo, Japan).

**Western blot analysis.** Adipose tissue of the mice was sectioned and homogenized, followed by centrifugation at 5,000  $\times$  g for 10 min at 4°C. The supernatant was collected and the protein concentration was determined using a Coomassie blue protein

Table I. Primer sequences of adipose tissue genes.

Genes	Primer sequence (5'-3')
Phosphoinositide 3-kinase	Forward: CGGTTTCTCCCTTCTACTTCCTG Reverse: GCTCTGCCTCAGCCTTTTATTG
Peroxisome proliferator-activated receptor $\gamma$	Forward: GCCCTTTGGTGACTTTATGGAG Reverse: TGTCCCCACATATTCGACACTC
Protein kinase B	Forward: GAAGACCCAAAGACCAAGATGC Reverse: TCTGACAACAAAGCAGGAGGTG
Insulin receptor	Forward: GTTGCCCTTCTTGGGACTGATGT Reverse: GGTCTGTTGTGGGTGGTATCCT
Insulin receptor substrate-1	Forward: CTTCTGTTACACCTCAAGGGGC Reverse: GGTTATGGTTGGGACTTAGGTTCA
Fatty acid synthetase	Forward: ACCTCATCACTAGGAAGCCACCAG Reverse: GTGGTACTTGGCCTTGGGTTTA
Adiponectin	Forward: CGTTCTCTTCACCTACGACCAGT Reverse: ATTGTTGTCCCCCTTCCCCATAC
Sterol regulatory element-binding protein 1	Forward: CCTGGAGCGAGCATTGAACT Reverse: ACTGACAGAGAAGCTGCACGC
$\beta$ -actin	Forward: ACGGTCAGGTCATCACTATCG Reverse: GGCATAGAGGTCTTTACGGATG

assay (Thermo Fisher Scientific, Inc.). Protein lysates (30  $\mu$ g) were then loaded in 19% SDS-PAGE, then transferred to polyvinylidene fluoride membranes (Merck KGaA, Darmstadt, Germany). Non-fat milk dissolved in tris-buffered saline with Tween-20 (0.1%; TBST) was used to block the membrane for 1 h at room temperature. The membranes were incubated overnight at 4°C with the following primary antibodies: IRS-1 Ser307 (1:800 dilution; cat. no. AI618; Beyotime Institute of Biotechnology, Shanghai, China), phosphorylated (p-) IRS1 Ser307 (1:800 dilution; cat. no. AI623-1; Beyotime Institute of Biotechnology), Akt (1:1,000 dilution; cat. no. 9272; Cell Signaling Technology, Inc., Danvers, MA, USA), p-Akt Ser473 (1:1,000 dilution; cat. no. 4060; Cell Signaling Technology, Inc.), PI3K (1:1,000 dilution; cat. no. 4249; Cell Signaling Technology, Inc.) and  $\beta$ -actin (1:50,000 dilution; cat. no. 3700; Cell Signaling Technology, Inc.). Subsequent to extensive washing (3 times) with TBST, horseradish peroxidase-conjugated goat anti-rabbit secondary antibodies (1:1,000; cat. no. ab150084; Abcam, Cambridge, UK) diluted in phosphate buffered saline were applied to the membrane followed by incubation for 1 h at room temperature. Subsequent to washing, enhanced chemiluminescence substrates (cat. no. 34580; Thermo Fisher Scientific, Inc.) were added to the membrane. Images of the membranes were analyzed using Quantity One 1-D analysis software (Bio-Rad Laboratories, Inc.).

**Immunohistochemistry.** Adipose tissue was fixed using 4% polyformaldehyde (Beijing Baiao Laibo Technology Co., Ltd., Beijing, China) for 20 min at room temperature and was sliced into 4  $\mu$ m-thick sections. Subsequent to dewaxing and hydration, these slices were soaked in 3% H<sub>2</sub>O<sub>2</sub> at room temperature for 10 min, followed by the repair of antigens by electric stove heating, and subsequently the following primary antibodies were added: p-IRS1 Ser307 (cat no. ab60946; 1:1,000; Abcam,

Cambridge, MA, USA) and p-Akt Ser473 (cat no. #4060; 1:100; Cell Signaling Technology, Inc.) and incubated for 30 min at 37°C. The horseradish peroxidase-conjugated secondary antibody-goat anti rabbit IgG (cat no. A0208; 1:50; Beyotime Institute of Biotechnology, Haimen, China) was added and incubated with specific antibody-binding capacity for 30 min at 37°C. Subsequent to staining with 3,3'-diaminobenzidine followed by counterstaining with hematoxylin and dehydration for 5 min, and the membranes were then treated with gradient alcohol for 10 min each then two changes of xylene for 3 min and sealed, all at room temperature. The samples were then observed under a Olympus BX51 fluorescence upright microscope (Olympus Corporation, Tokyo, Japan).

**Statistical analysis.** Data were represented as the mean  $\pm$  the standard deviation, and analyzed using SPSS 19.0 (IBM Corp., Armonk, NY, USA). Comparisons among different groups were based on one-way analysis of variance analysis. Paired comparisons between different groups were performed using the Student Newman Keul's method.  $P < 0.05$  was considered to indicate a statistically significant difference.

## Results

**Effect of dioscin on the phenotypic parameters of mice.** Subsequent to being fed with high-fat food for 12 weeks, biochemical parameters, including initial body mass, final body mass, total fat and adiposity index, were significantly increased compared with the control group ( $P < 0.05$ ; Table II). Compared with the HFD group, mice in the medium and high dioscin groups were revealed to have significantly decreased levels of final body weight, and in all three dioscin groups had significantly decreased levels of total fat and adiposity index in a dose-dependent manner ( $P < 0.05$ ).

Table II. Phenotypic parameters of mice in different groups.

Parameter	Group				
	Control	High-fat diet	Dioscin (low)	Dioscin (medium)	Dioscin (high)
Initial body mass (g)	20.8±0.6	21.1±0.4	20.7±0.3	21.3±0.5	20.4±0.7
Final body mass (g)	29.2±0.7	40.3±1.1 <sup>a</sup>	38.2±1.2	34.9±0.9 <sup>c</sup>	31.5±0.8 <sup>c</sup>
Total fat (g)	0.77±0.04	8.07±0.13 <sup>b</sup>	6.94±0.15 <sup>c</sup>	5.38±0.11 <sup>c</sup>	2.91±0.07 <sup>d</sup>
Adiposity index (%)	2.51±0.41	20.45±0.58 <sup>b</sup>	17.21±0.43 <sup>c</sup>	15.08±0.52 <sup>c</sup>	9.37±0.37 <sup>c</sup>

<sup>a</sup>P<0.05 and <sup>b</sup>P<0.01 vs. the control group; <sup>c</sup>P<0.05 and <sup>d</sup>P<0.01 vs. the high-fat diet group.

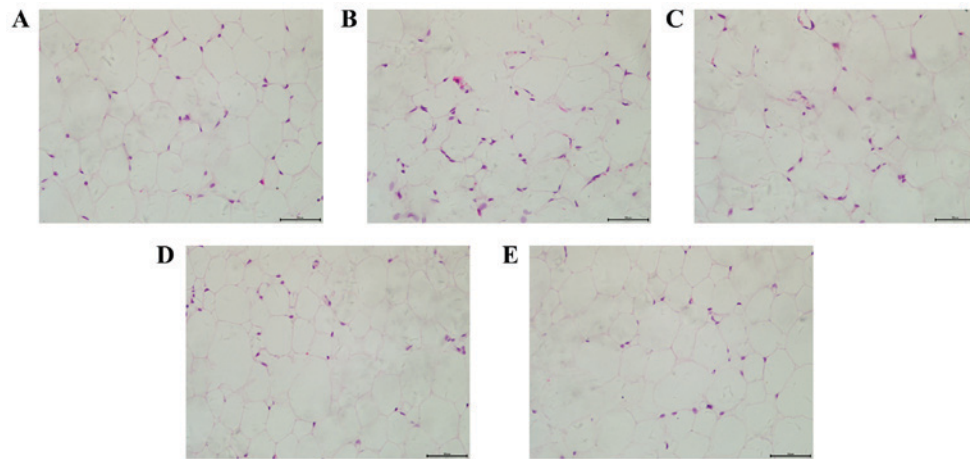


Figure 1. Pathological analysis of adipose tissue by H&E staining (magnification, x200). Representative H&E staining of adipose tissue from mice in (A) the control group, (B) a high-fat diet group, (C) a low dioscin treatment group, (D) a medium dioscin treatment group and (E) a high dioscin treatment group. H&E, hematoxylin and eosin.

**Effects of dioscin on the pathology changes of adipose cells.** H&E staining was applied to detect the morphology of adipose cells in a number of different groups. As presented in Fig. 1, mice in the HFD group demonstrated an increased volume and decreased number of adipose cells, accompanied with a more varied shape and size of cells compared with the control group. However, dioscin treatment attenuated the morphological changes of adipose cells, further demonstrating the effect of dioscin on restoring the phenotypic parameters in a HFD model.

**Regulation of insulin resistance by dioscin.** Next, the present study examined whether dioscin reduced insulin resistance by evaluating the changes of biochemical parameters of the serum obtained from the mice. As presented in Table III, mice fed with a HFD demonstrated a significant elevation of blood glucose, insulin, TC, TG and NEFA levels when compared with the control group ( $P<0.05$ ), resulting in significantly higher HOMA-IR and Adipo-IR values ( $P<0.01$ ; Table III). Notably, dioscin treatment significantly lowered HOMA-IR ( $P<0.05$ ) and Adipo-IR levels ( $P<0.01$ ) in a dose-dependent manner.

**Effects of dioscin on the IRS-1/PI3K/Akt and PPAR $\gamma$  signaling pathway.** To better understand the underlying mechanisms of dioscin, the present study examined the

potential cell signal pathways involved and revealed that a HFD significantly downregulated the mRNA levels of PI3K, Akt, insulin receptor (IR) and IRS-1 ( $P<0.05$ ; Fig. 2), when compared with the control group, whilst the high dioscin treatment group exhibited a significant effective restoration of the aberrant expression of the aforementioned genes ( $P<0.05$ ; Fig. 2). Interestingly, it was additionally revealed that dioscin may significantly reverse the decrease in the expression of PPAR $\gamma$  incurred by a HFD treatment ( $P<0.05$ ; Fig. 3A) with no prominent regulation effects on the levels of FAS, adiponectin and SREBP-1c (Fig. 3B-D).

Furthermore, p-IRS-1 and IRS-1 levels were examined by western blot analysis. As presented in Fig. 4A, a HFD significantly upregulated the p-IRS1/IRS-1 ratio compared with the control group ( $P<0.01$ ), and dioscin at doses of 10 and 20 mg/kg/day significantly reduced this value compared with the HFD group ( $P<0.05$ ). Meanwhile, p-Akt/Akt value was significantly decreased in the HFD group in comparison with the control group ( $P<0.05$ ; Fig. 4B). In contrast, a high dose of dioscin significantly increased the p-Akt/Akt value compared with the HFD group ( $P<0.05$ ; Fig. 4B).

**Immunohistochemical analysis.** The results of the immunohistochemical analysis were consistent with the results of the western blot analysis in Figure 5. Immunohistochemical staining revealed that the levels of p-IRS1 and p-Akt proteins



Table III. Biochemical parameters of plasma.

Parameters	Groups				
	Control	High-fat diet	Dioscin (low)	Dioscin (medium)	Dioscin (high)
Plasma glucose (mg/dl)	106.77±7.92	131.93±9.17 <sup>a</sup>	124.39±6.53	118.94±5.23 <sup>c</sup>	111.34±7.30 <sup>c</sup>
Plasma insulin (ng/ml)	0.34±0.07	2.41±0.21 <sup>b</sup>	1.93±0.25	1.53±0.17 <sup>c</sup>	0.90±0.11 <sup>d</sup>
Triglyceride (mg/dl)	51.69±5.16	90.47±7.08 <sup>b</sup>	79.21±5.93	68.38±5.02 <sup>c</sup>	59.07±6.17 <sup>d</sup>
Total cholesterol (mg/dl)	68.39±5.33	89.04±7.48 <sup>a</sup>	78.38±6.47	72.79±6.09 <sup>c</sup>	70.33±5.73 <sup>c</sup>
Non-esterified fatty acids (mEq/l)	0.95±0.11	1.45±0.15 <sup>a</sup>	1.28±0.20	1.19±0.18	1.04±0.10 <sup>c</sup>
Homeostasis model assessment of insulin resistance index	2.15±0.24	18.79±1.96 <sup>b</sup>	14.19±1.33	10.75±1.06 <sup>c</sup>	6.03±0.79 <sup>c</sup>
Adipose insulin resistance index	55.61±6.76	601.70±19.05 <sup>b</sup>	425.37±16.38 <sup>c</sup>	313.50±15.79 <sup>d</sup>	161.17±17.23 <sup>d</sup>

<sup>a</sup>P<0.05 and <sup>b</sup>P<0.01 vs. the control group. <sup>c</sup>P<0.05 and <sup>d</sup>P<0.01 vs. the high-fat diet group.

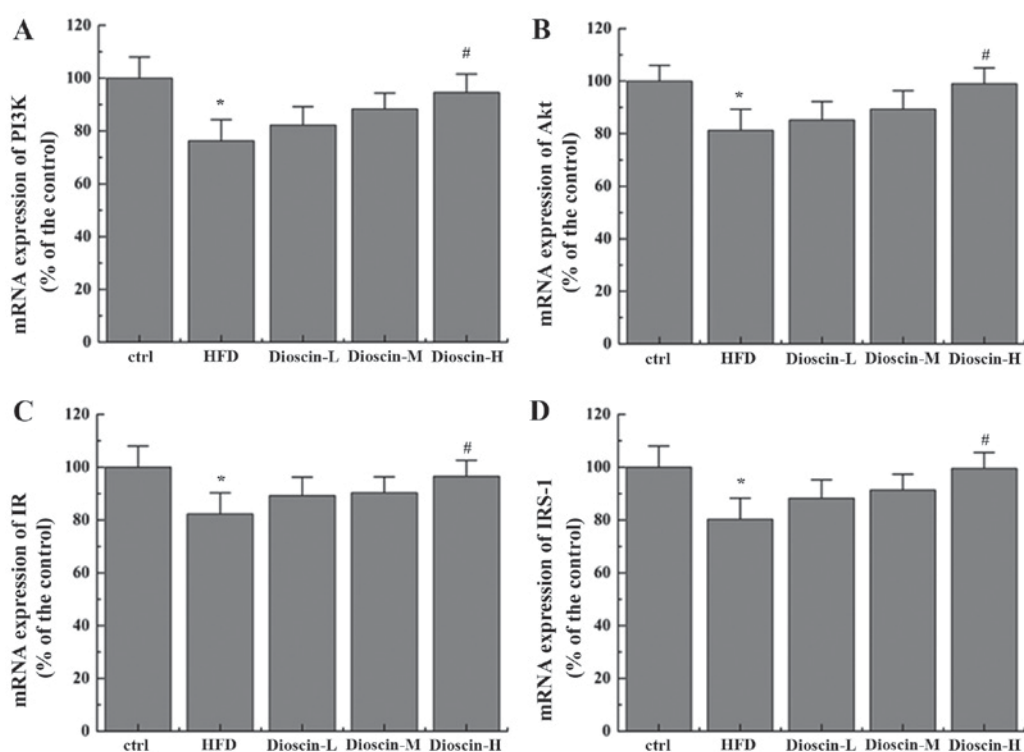


Figure 2. Effects of dioscin on the expression of genes in the IRS-1/PI3 K/Akt pathway. The relative mRNA levels of (A) PI3K, (B) Akt, (C) IR and (D) IRS-1 were presented. \*P<0.05 vs. the ctrl group; #P<0.05 vs. the HFD group. IRS-1, insulin receptor substrate 1; PI3K, phosphoinositide 3-kinase; IR, insulin receptor; Akt, protein kinase B; HFD, high-fat diet; ctrl, control; L, low; M, medium; H, high.

in the adipose tissue of the model group were substantially up- and downregulated, respectively, compared with the control group. Subsequent to treated using dioscin, the protein expression of p-IRS1 decreased, and the expression of p-Akt increased compared with the HFD group. The higher the concentration of dioscin, the more substantial the phosphorylation of IRS1 and Akt appeared to be.

## Discussion

The results of the present study were in agreement with a previous report that dioscin potently reduced obesity in mice, and may be explained by the fact that dioscin elevates

the energy expenditure in obese mice (9). HFD impairs fatty acid synthesis and metabolism in the liver, which increases TG levels and various other molecules in TG synthesis. The present study revealed that dioscin is effective in attenuating the increased body weight and body fat induced by HFD. Upon dioscin treatment, a reduction of plasma glucose, TG and plasma insulin levels was also observed, suggesting the amelioration of liver injuries caused by HFD and ameliorated insulin resistance, as reflected by the decrease in HOMA-IR and Adipo-IR indexes, in addition to the increase in adipose cell volume and decrease in adipose cell number, which corroborated the potential use of dioscin in the clinical management of insulin resistance.

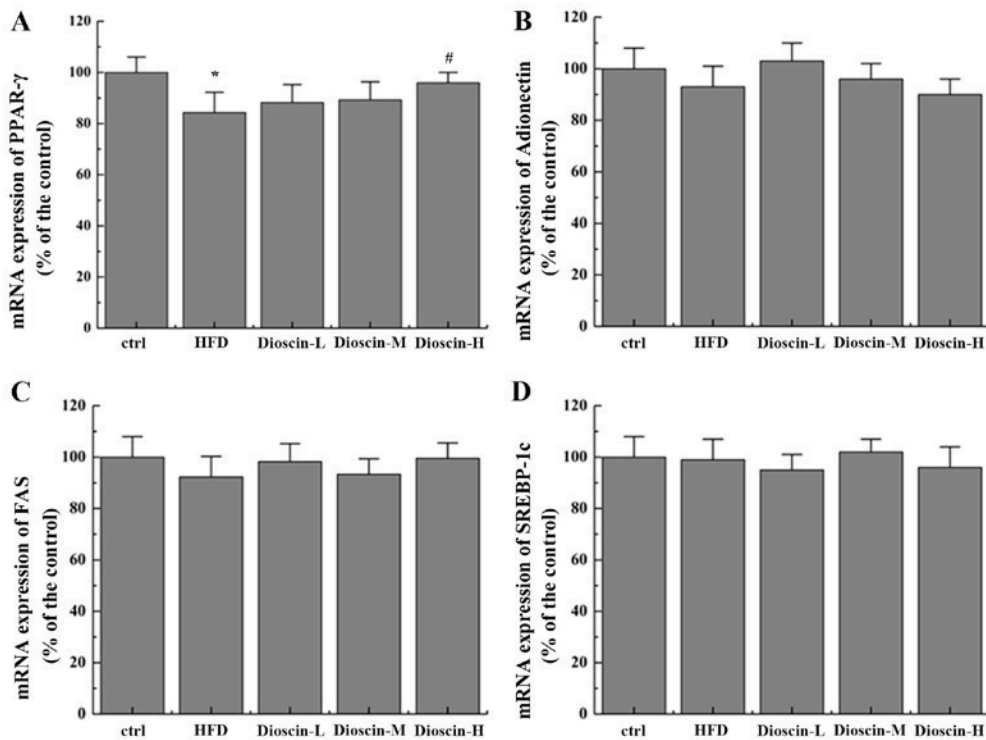


Figure 3. Effects of dioscin on the expression of genes in the PPAR- $\gamma$  pathway. Relative mRNA levels of (A) PPAR- $\gamma$ , (B) adiponectin, (C) FAS and (D) SREBP-1c were determined. \* $P < 0.05$  vs. the ctrl group; # $P < 0.05$  vs. the HFD group. PPAR- $\gamma$ , Peroxisome proliferator-activated receptor  $\gamma$ ; FAS, fatty acid synthetase; SREBP-1c, sterol regulatory element-binding protein 1; HFD, high-fat diet; ctrl, control; L, low; M, medium; H, high.

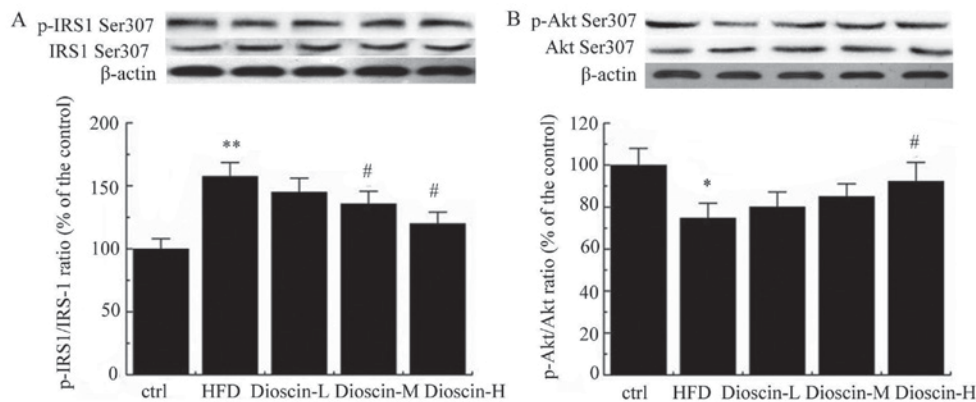


Figure 4. Western blot analysis of p-IRS-1/IRS-1 and p-Akt/Akt. Protein expression of (A) p-IRS1, IRS-1, (B) p-Akt and Akt measured using western blot analysis. \* $P < 0.05$  and \*\* $P < 0.01$  vs. the ctrl group; # $P < 0.05$  vs. the HFD group. P-, phosphorylated; IRS-1, insulin receptor substrate-1; Akt, protein kinase B; ctrl, control; HFD, high-fat diet; L, low; M, medium; H, high.

In the present study, it was revealed that dioscin regulated PI3K/Akt signaling in HFD mice. A HFD was able to significantly downregulate the level of PI3K and Akt compared with the control group ( $P < 0.05$ ), while dioscin demonstrated a dose-dependent effect on the increased expression of PI3K, Akt, IR and IRS-1, particularly in the 20 mg/kg/day group. The inhibition of IRS-1 and Akt signaling was mediated through the phosphorylation (Ser307) of the proteins. The aforementioned result is preceded by results that indicate that insulin resistance is activated by the inhibition of Akt and IRS-1 substrate phosphorylation (15,16). IRS-1 is one of the key targets of the insulin receptor tyrosine kinase, which is indispensable for the activation of downstream metabolism. Insulin specifically binds to the  $\alpha$  subunit of insulin receptor in the cell surface and

activates the  $\beta$  subunit inhibited by the  $\alpha$  subunit, resulting in phosphorylation under the action of tyrosine kinase, activation of IRS and the further cascade reaction of downstream activation signals, including the PI3K/Akt and mitogen-activated protein kinase signaling pathway (17). The ability of dioscin to reverse the blockage of IRS-1-associated signaling improved the sensitivity of adipose tissue to insulin. This result is consistent with evidence that numerous saponins are also effective in ameliorating insulin resistance by modulating the PI3K/Akt signaling pathway (11,18,19). The PI3K/Akt and PPAR- $\gamma$  pathways are the two putative pathways that are suppressed in diseases associated with excessive oxidative stress and inflammation (15,18-20). The restoration of the activity of those two pathways, and consequent amelioration of oxidative

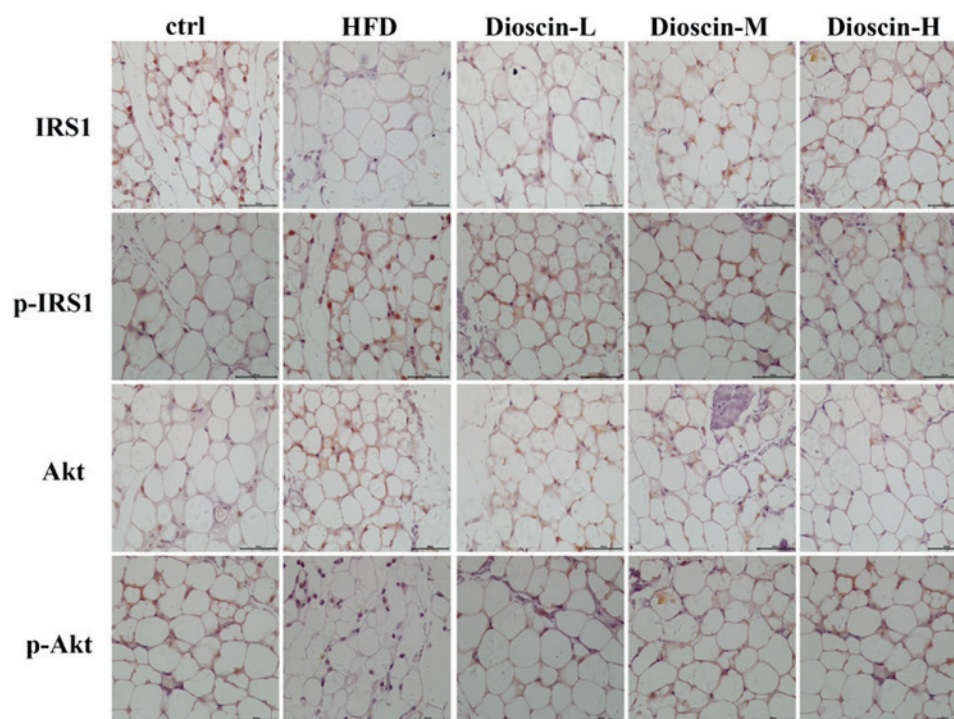


Figure 5. Protein expression of p-IRS1 and p-Akt analyzed using an immunohistochemical assay (magnification, x400). P-, phosphorylated; IRS-1, insulin receptor substrate-1; Akt, protein kinase B; ctrl, control; HFD, high-fat diet; L, low; M, medium; H, high.

and inflammatory responses, may potentially account for the effects of dioscin on mitigating insulin resistance. In 2013, Gao *et al* (20) reported that *Ginsenoside Re* may reduce insulin resistance through the activation of the PPAR- $\gamma$  pathway and inhibition of tumor necrosis factor- $\alpha$  (TNF- $\alpha$ ) production. In 2018, Naowaboot *et al* (21) reported that the administration of a water extract of *V cinerea* was able to increase insulin sensitivity in HFD-induced obese mice by modulating the PI3K/Akt and AMPK pathways in the liver, skeletal muscle and adipose tissue. Additionally, Cai *et al* (22) reported that *Sangua Drink* extract may alleviate insulin resistance in treating type 2 diabetes mellitus rats induced by a HFD through the PI3K/Akt signaling pathway. Furthermore, Leng *et al* (23) reported that 1,1,2-Trichloro-1,2,2-trifluoroethane may regulate macrophage polarization with beneficial effects on adipose tissue inflammation, and thereby facilitate insulin IRS-1/PI3K signaling, resulting in the improvement of insulin sensitivity in HFD-fed mice. Further biochemical analysis on factors associated with oxidative stress, including levels of malondialdehyde and glutathione, in addition to inflammatory responses including interleukin-1 and TNF- $\alpha$ , is necessary to confirm this assumption. It is also worth noting that dioscin did not demonstrate a significant impact on the expression of FAS, adiponectin and SREBP-1c, which are factors associated with insulin-sensitization or fatty acid synthesis (24), suggesting that dioscin did not ameliorate insulin resistance in adipose tissue through those mechanisms.

In summary, the present study demonstrated that dioscin is a promising drug for the treatment of insulin resistance. In addition, reduced body weight and serum FFA levels determined dioscin as an excellent candidate in the treatment of other obesity-induced disorders. For example, a HFD and obesity are two risk factors of cardiovascular disease, as high fatty acid

levels promote endothelial dysfunction, ultimately resulting in atherosclerosis and coronary artery diseases (25). The effects of dioscin on reducing body weight and serum FFA may benefit the prevention and treatment of cardiovascular diseases. Consequently, it was hypothesized that dioscin is beneficial in regulating the abnormal metabolism of obese mice, restoring the activity of the IRS-1/PI3K/Akt pathway and PPAR- $\gamma$  pathway, in order to reverse the insulin resistance induced by a HFD.

#### Acknowledgements

Not applicable.

#### Funding

No funding was received.

#### Availability of data and materials

All data generated or analyzed during this study are included in this published article.

#### Authors' contributions

HL, LY and CZ conceived designed and performed the experiments. HL, LY and CZ analyzed the data and prepared the manuscript. All authors read and approved the final version of the manuscript.

#### Ethics approval and consent to participate

The present study was approved by the Ethics Committee of The Affiliated Yantai Yuhuangding Hospital of Qingdao

University (Yantai, China), and all participants provided written informed consent.

### Patient consent for publication

All participants provided written informed consent.

### Competing interests

The authors declare that they have no competing interests.

### References

- Samuel VT and Shulman GI: Mechanisms for insulin resistance: Common threads and missing links. *Cell* 148: 852-871, 2012.
- Turner N, Kowalski GM, Leslie SJ, Risis S, Yang C, Lee-Young RS, Babb JR, Meikle PJ, Lancaster GI, Henstridge DC, *et al*: Distinct patterns of tissue-specific lipid accumulation during the induction of insulin resistance in mice by high-fat feeding. *Diabetologia* 56: 1638-1648, 2013.
- Tao X, Yin L, Xu L and Peng J: Dioscin: A diverse acting natural compound with therapeutic potential in metabolic diseases, cancer, inflammation and infections. *Pharmacol Res* (In press).
- Kim S, Jwa H, Yanagawa Y and Park T: Extract from *dioscorea batatas* ameliorates insulin resistance in mice fed a high-fat diet. *J Med Food* 15: 527-534, 2012.
- Aumsuwan P, Khan SI, Khan IA, Ali Z, Avula B, Walker LA, Shariat-Madar Z, Helferich WG, Katzenellenbogen BS and Dasmahapatra AK: The anticancer potential of steroidal saponin, dioscin, isolated from wild yam (*Dioscorea villosa*) root extract in invasive human breast cancer cell line MDA-MB-231 in vitro. *Arch Biochem Biophys* 591: 98-110, 2016.
- Liu C, Wang Y, Wu C, Pei R, Song J, Chen S and Chen X: Dioscin's antiviral effect in vitro. *Virus Res* 172: 9-14, 2013.
- Guo CH, Li X and Kang Y: The protective effect of dioscin-containing serum on hydrogen peroxide injured cardiomyocytes of neonate rats. *Chin J Hosp Pharm* 13: 1027-1031, 2012 (In Chinese).
- Tao X, Wan X, Xu Y, Xu L, Qi Y, Yin L, Han X, Lin Y and Peng J: Dioscin attenuates hepatic ischemia-reperfusion injury in rats through inhibition of oxidative-nitrative stress, inflammation and apoptosis. *Transplantation* 98: 604-611, 2014.
- Liu M, Xu L, Yin LH, Qi Y, Xu Y, Han X, Zhao Y, Sun H, Yao J, Lin Y, *et al*: Corrigendum: Potent effects of dioscin against obesity in mice. *Sci Rep* 5: 12183, 2015.
- Kwon H and Pessin JE: Adipokines mediate inflammation and insulin resistance. *Front Endocrinol (Lausanne)* 4: 71, 2013.
- Hu X, Wang S, Xu J, Wang DB, Chen Y and Yang GZ: Triterpenoid saponins from *Stauntonia chinensis* ameliorate insulin resistance via the AMP-activated protein kinase and IR/IRS-1/PI3K/Akt pathways in insulin-resistant HepG2 cells. *Int J Mol Sci* 15: 10446-10458, 2014.
- Gallagher EJ, Fierz Y, Vijayakumar A, Haddad N, Yakar S and LeRoith D: Inhibiting PI3K reduces mammary tumor growth and induces hyperglycemia in a mouse model of insulin resistance and hyperinsulinemia. *Oncogene* 31: 3213-3222, 2012.
- Hsieh MJ, Tsai TL, Hsieh YS, Wang CJ and Chiou HL: Dioscin-induced autophagy mitigates cell apoptosis through modulation of PI3K/Akt and ERK and JNK signaling pathways in human lung cancer cell lines. *Arch Toxicol* 87: 1927-1937, 2013.
- Livak KJ and Schmittgen TD: Analysis of relative gene expression data using real-time quantitative PCR and the 2(-Delta Delta C(T)) method. *Methods* 25: 402-408, 2001.
- Plomgaard P, Bouzakri K, Krogh-Madsen R, Mittendorfer B, Zierath JR and Pedersen BK: Tumor necrosis factor- $\alpha$  induces skeletal muscle insulin resistance in healthy human subjects via inhibition of Akt substrate 160 phosphorylation. *Diabetes* 54: 2939-2945, 2005.
- Copps KD and White MF: Regulation of insulin sensitivity by serine/threonine phosphorylation of insulin receptor substrate proteins IRS1 and IRS2. *Diabetologia* 55: 2565-2582, 2012.
- Guo S: Insulin signaling, resistance, and the metabolic syndrome: Insights from mouse models into disease mechanisms. *J Endocrinol* 220: T1-T23, 2014.
- Hu X, Wang M, Bei W, Han Z and Guo J: The Chinese herbal medicine FTZ attenuates insulin resistance via IRS1 and PI3K in vitro and in rats with metabolic syndrome. *J Transl Med* 12: 47, 2014.
- Zhang Y, Hai J, Cao M, Zhang Y, Pei S, Wang J and Zhang Q: Silibinin ameliorates steatosis and insulin resistance during non-alcoholic fatty liver disease development partly through targeting IRS-1/PI3K/Akt pathway. *Int J Immunopharmacol* 17: 714-720, 2013.
- Gao Y, Yang MF, Su YP, Jiang HM, You XJ, Yang YJ and Zhang HL: Ginsenoside Re reduces insulin resistance through activation of PPAR- $\gamma$  pathway and inhibition of TNF- $\alpha$  production. *J Ethnopharmacol* 147: 509-516, 2013.
- Naowaboot J, Wannasiri S and Pannangpetch P: Vernonia cinerea water extract improves insulin resistance in high-fat diet-induced obese mice. *Nutr Res* 56: 51-60, 2018.
- Cai Y, Wang Y, Zhi F, Xing QC and Chen YZ: The effect of sanggaa drink extract on insulin resistance through the PI3K/AKT signaling pathway. *Evid Based Complement Alternat Med* 2018: 9407945, 2018.
- Leng J, Chen MH, Zhou ZH, Lu YW, Wen XD and Yang J: Triterpenoids-enriched extract from the aerial parts of *salvia miltiorrhiza* regulates macrophage polarization and ameliorates insulin resistance in high-fat fed mice. *Phytother Res* 31: 100-107, 2017.
- Ranganathan G, Unal R, Pokrovskaya I, Yao-Borengasser A, Phanavanh B, Lecka-Czernik B, Rasouli N and Kern PA: The lipogenic enzymes DGAT1, FAS, and LPL in adipose tissue: Effects of obesity, insulin resistance, and TZD treatment. *J Lipid Res* 47: 2444-2450, 2006.
- Liu K, Zhao W, Gao X, Huang F, Kou J and Liu B: Diosgenin ameliorates palmitate-induced endothelial dysfunction and insulin resistance via blocking IKK $\beta$  and IRS-1 pathways. *Atherosclerosis* 223: 350-358, 2012.